Machine learning identifies potential diagnostic biomarkers associated with ferroptosis in obstructive sleep apnea

BOWEN CHEN, LIPING DONG, WEIWEI CHI and DONGMEI SONG

Clinical Biobank, The First Hospital of Hebei Medical University, Hebei Medical University, Shijiazhuang, Hebei 050031, P.R. China

Received November 11, 2024; Accepted February 6, 2025

DOI: 10.3892/etm.2025.12845

Abstract. Obstructive sleep apnea (OSA) is the most common sleep apnea-related disorder, with a high prevalence and a range of associated complications. Ferroptosis is a new mode of cell death that is involved in the development of OSA, but the mechanism has remained elusive. In the present study, ferroptosis-related genes in OSA were assessed and their potential clinical value was discussed. Data were downloaded and merged, and screened for differentially expressed genes (DEGs) through the Gene Expression Omnibus database. The OSA ferroptosis-related genes were obtained after intersecting with the downloaded ferroptosis-related genes. Subsequently, key ferroptosis-associated differential genes were obtained using two machine learning methods (the least absolute shrinkage and selection operators and random forest). The immune infiltration in the samples and the correlation between key differential genes and immune infiltrating cells were then analyzed. A competing endogenous (ce)RNA visualization network was constructed to find possible therapeutic targets. Finally, the expression levels of key DEGs were verified by reverse transcription-quantitative (RT-q)PCR. In this study, 3 key ferroptosis-related differential genes were identified: TXN, EGR1 and CDKN1A. Functional enrichment analysis showed that the three key differential genes in OSA can influence the development of OSA by affecting metabolism, immune response and other processes. RT-qPCR experiments verified the expression of these key genes, further confirming the findings. A persistent state of immune activation may promote the progression of OSA, with marked infiltration of T cells and natural killer cells in OSA tissues. Genipin is a possible targeted therapeutic agent for OSA. Meanwhile, ceRNA network analysis identified several long non-coding RNAs that can regulate OSA disease progression. A total of 3 key ferroptosis-related markers were identified (TXN, EGR1 and CDKN1A) that are closely associated with metabolic disorders and immune responses, and which may be targets for early diagnosis and treatment of OSA.

Correspondence to: Professor Dongmei Song, Clinical Biobank, The First Hospital of Hebei Medical University, Hebei Medical University, 89 Dong Gang Road, Shijiazhuang, Hebei 050031, P.R. China
E-mail: songdongmei@hebmu.edu.cn

Abbreviations: OSA, obstructive sleep apnea; DEGs, differentially expression genes; GEO, Gene Expression Omnibus; ceRNA, competing endogenous RNA; WGCNA, weighted gene co-expression network; LASSO, least absolute shrinkage and selection operators; RF, random forest; PCA, principal component analysis; GO, Gene Ontology; KEGG, Kyoto Encyclopedia of Genes and Genomes; AUC, area under the curve; ROC, receiver operating characteristic; PBMCs, peripheral blood mononuclear cells; RT-qPCR, reverse transcription-quantitative PCR

Key words: obstructive sleep apnea, ferroptosis, bioinformatics, immune-related genes, targeted therapy, machine learning

Introduction

Obstructive sleep apnea (OSA) is a clinical condition characterized by complete or partial collapse of the upper airway during sleep, resulting in reduced intrathoracic pressure, intermittent hypoxia and sleep disturbances (1), and it is an important risk factor for cardiovascular disease and mortality (2,3). The prevalence of OSA is high (4), affecting 20-30% of the general population (5), nearly 1 billion individuals worldwide (6). Currently, the treatment for OSA relies on lifestyle changes, ventilator therapy and surgery; however, these treatments are either poorly adhered to by patients or are costly, traumatic and do not change the nature of the disease. Therefore, it is necessary to explore the mechanisms of OSA occurrence and progression and to identify targeted therapeutics that allow for the early prevention and treatment of OSA.

OSA-induced apoptosis has been the focus of previous studies and ferroptosis is a form of programmed cell death distinct from apoptosis and necrosis, characterized by the lethal accumulation of lipid peroxides (7,8). When the cellular cysteine transporter is inhibited, the reduction of intracellular glutathione can lead to the accumulation of lipid peroxidation, which can induce cellular ferroptosis after reaching a certain level. Previous studies have shown that iron death plays a key role in the pathology of the development of diseases such as myocardial infarction, stroke, cerebral ischemia, autoimmune diseases, respiratory diseases and cancer (9). Studies have shown that the administration of iron death inhibitors in diseased tissues reduces the observed cell death and that control of iron death may influence disease onset and progression (10). Therefore, exploring the role

of iron death in various diseases by data screening of iron death-related genes is important for the prevention and treatment of these diseases. Ferroptosis has been found to play an important role in OSA-induced myocardial injury, liver injury and cognitive impairment in previous studies (11-13), suggesting that inhibition of ferroptosis is a new direction for combating the progression of OSA. Therefore, it is important to explore the mechanism of ferroptosis in patients with OSA and find specific diagnostic markers related to ferroptosis for the diagnosis and treatment of OSA.

With the rapid development of bioinformatics, compared with time-consuming and expensive traditional experimental studies, bioinformatics analysis can screen a large number of potentially valuable genes faster and more accurately, and provide exploratory predictions at a much lower cost to inform subsequent biological experiments and clinical applications (14). Machine learning is an important branch of bioinformatics that has significant advantages in handling large amounts of data. Machine learning algorithms are capable of automatically extracting valuable information from massive data, improving prediction accuracy and real-time decision support. In this paper, a bioinformatics approach was used to collect data from the Gene Expression Omnibus (GEO) database to screen for differentially expressed genes (DEGs), followed by functional/pathway enrichment analysis, weighted gene co-expression network analysis (WGCNA) and module analysis and genomic enrichment analysis (GSEA). This was followed by screening of key biomarkers using two methods of machine learning: the least absolute shrinkage and selection operator (LASSO) and random forest (RF). In addition, the expression levels and diagnostic value of the key differential genes were analyzed and the expression levels of key biomarkers were examined in mononuclear cells collected from patient blood samples. Finally, the prediction of targeted drugs for key marker genes and a competing endogenous (ce)RNA network analysis identified some long non-coding (lnc)RNAs that can regulate the disease progression of OSA. Using these data, the study aimed to explore new potential diagnostic and therapeutic targets for patients with OSA. The flowchart of this study design is shown in Fig. 1.

Materials and methods

Data acquisition and processing. The GEO database (http://www.ncbi.nlm.nih.gov/geo/) was used to search and download qualified expression datasets. The datasets GSE135917 (https://www.ncbi.nlm.nih.gov/geo/query/acc.cgi?acc=GSE135917) and GSE38792 (https://www.ncbi.nlm.nih.gov/geo/query/acc.cgi?acc=GSE38792) were used for the present study. The annotation information was transformed into a gene expression matrix by means of a platform file. The GSE135917 and GSE38792 data were also merged using the 'sva' package of the R software (version 4.2.1; https://cran.r-project.org/bin/windows/base/). Specific information about batch effects was visualized by principal component analysis (PCA). The gene list file for ferroptosis-related genes downloaded from the Ferrdb v2 database (http://www.zhounan.org/ferrdb/current/) on June 28, 2023 comprised a total of 484 genes (drivers, suppressors and markers).

Screening for differential expression. DEGs were identified from the merged dataset. The 'limma' R package was used to screen DEGs and |log2 fold change (FC)|>0.5 and adjusted P<0.05 were selected as the cut-off standard. The 'ggplot2' package was employed for creating the volcano map to visualize these DEGs. The 'pheatmap' package was used to create a heat map of DEGs and screen for expression differences between the experimental and control groups. The genes in the overlap between the differential genes and the ferroptosis-related genes were considered the OSA ferroptosis-related differential genes.

Functional and pathway enrichment analyses. Gene Ontology (GO) terms were determined and a Kyoto Encyclopedia of Genes and Genomes (KEGG) pathway enrichment analysis of DEGs associated with ferroptosis was performed using clusterProfiler. Terms were derived from KEGG pathway and GO analyses, including functional terms in the categories molecular function, biological process and cellular components. To select the relevant pathways, the adjusted statistical threshold criteria of P<0.05 were used. Finally, important signaling pathways were further explored using the clusterProfile package and the gene set variation analysis (GSVA) package from the R software. The gene expression matrix of OSA was analyzed by GSEA to explore its possible regulatory pathways. In addition, function and pathway files containing mainly GSVA scores of the corresponding functional pathways were obtained for each sample. The 'limma' package was used to compare the GSVA scores of OSA and normal samples and the criteria for screening differential GSVA scores were P<0.05 and |log FC|>0.2 (15).

Construction and module analysis of WGCNA. WGCNA is a bioinformatics analysis method used to describe gene association patterns among different samples. The WGCNA software package in R.4.2.1 was used to perform WGCNA analysis. The WGCNA R package was utilized to construct a co-expression network corresponding to the clinical features of DEGs in OSA. First, hierarchical clustering analysis was performed using the Hclust function in R to exclude outlier samples. Subsequently, according to the criteria of a scale-free network, the 'pickSoftThreshold' function in the WGCNA software package was utilized to select the appropriate soft power β (ranging from 1 to 20) for automatic network construction. The results were clustered by topological overlap matrix analysis, which contains module assignments labeled by color and module eigengene (ME). In addition, Pearson correlation analysis was used to calculate the correlation between ME and clinical features. Modules with R>0.3 and P<0.05 were considered significant in terms of the interaction with clinical features.

Screening of feature genes. Disease prediction was performed using two machine learning algorithms to identify significant key marker genes. LASSO is an important method for regression that uses an l1 penalty to achieve a sparse solution (16). RF is a machine learning method that provides higher accuracy, sensitivity and specificity compared with traditional machine learning methods such as single decision tree (17), logistic regression (18) and K-nearest neighbor (19). It can

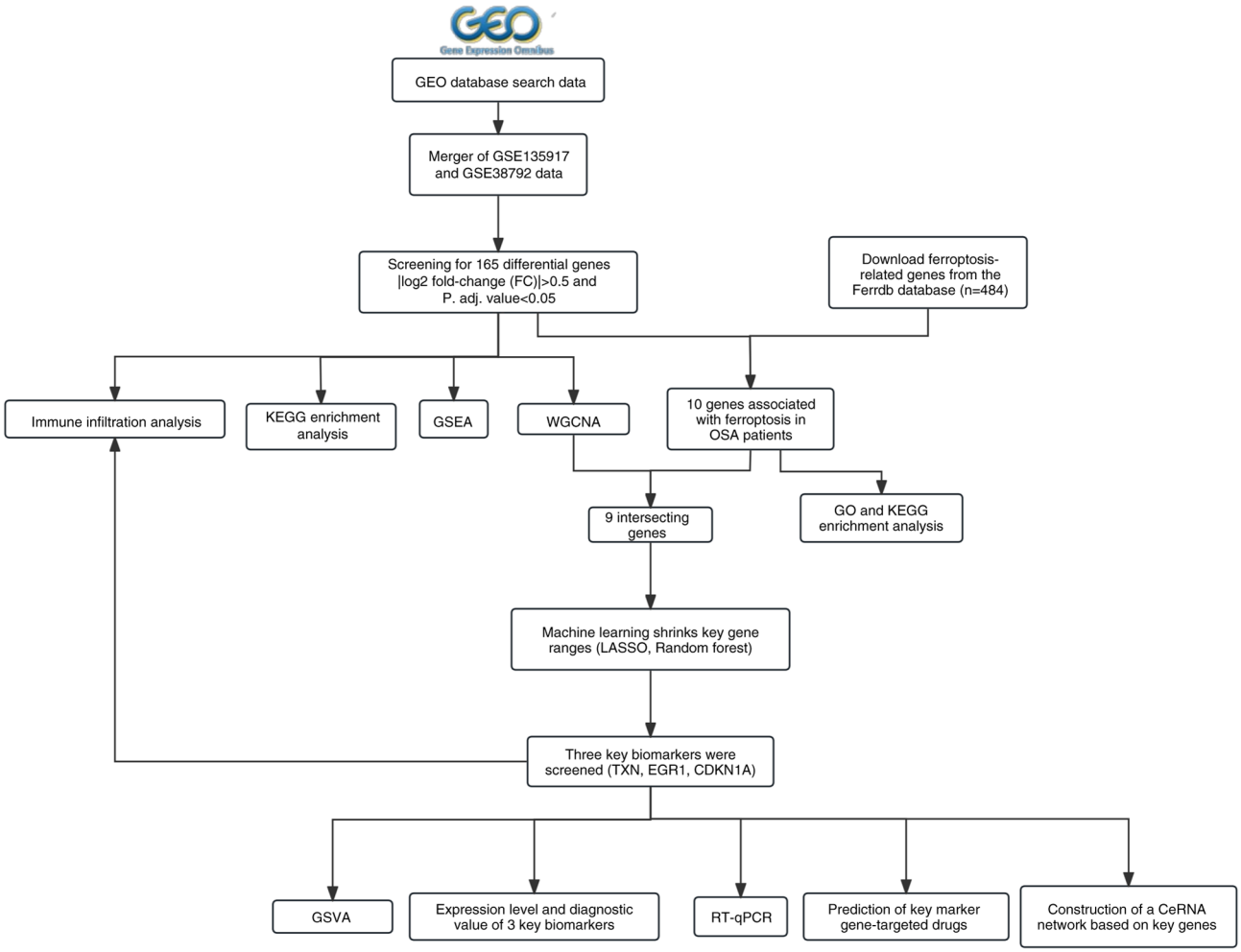

Figure 1. Study flowchart. GEO, gene expression omnibus; WGCNA, weighted gene co-expression network analysis; DEG, differentially expressed gene; LASSO, the least absolute shrinkage and selection operators; adj., adjusted; KEGG, Kyoto Encyclopedia of Genes and Genomes; GO, Gene Ontology; ceRNA, competing endogenous RNA; RT-qPCR, reverse transcription-quantitative PCR; GSVA, gene set variation analysis; GSEA, gene set enrichment analysis; OSA, obstructive sleep apnea.

be used to predict continuous variables and provide predictions without significant differences (20). The 'glmnet' (21) and 'randomForest' (22) R packages were used to perform LASSO regression and RF analysis. The intersection of the genes screened by LASSO and the genes screened by RF were measured and the shared genes were considered as candidate hub genes.

Candidate biomarker expression levels and diagnostic value. The expression levels of key shared genes in the GSE135917 dataset were detected using the ggplot2 package of R software ($P<0.05$ was considered statistically different in the OSA group compared to the control group) and the corresponding box plots were plotted using R software. The area under the curve (AUC) of the receiver operating characteristic (ROC) was utilized to determine the diagnostic value of potential biomarkers in the combined dataset using the pROC R package.

Single-sample (ss)GSEA. ssGSEA analysis was performed using the 'GSVA' R package to analyze the infiltration of 28 immune cells in lesions and normal samples. To analyze the association between immune cell content and feature gene expression, the 'ggplot2' package was used for correlation analysis and visualization. The relationship between feature genes and differentially infiltrating immune cells was investigated using Spearman correlation analysis. Pearson's correlation coefficient ($r>0.6$ and $P<0.05$ were used to verify the correlation between the feature genes and immune infiltrating cells.

Drug regulatory network. The Drug Gene Interaction Database (DGIdb; https://dgidb.org/) is used to predict drugs that interact with hub genes. An online tool called Cytoscape (https://cytoscape.org/) was used to construct interaction networks between potential drugs and hub genes and visualize the results.

Constructing ceRNA networks. Three databases were used to predict miRNA target genes, including miRanda (http://www.microrna.org/microrna/home.do), miRDB (http://mirdb.org/) and TargetScan (http://www.targetscan.org/). LncRNA-miRNA interactions were predicted by the spongeScan database (http://spongescan.rc.ufl.edu/). Cytoscape was used to construct ceRNA networks.

Extraction of peripheral blood mononuclear cells (PBMC). Between May and June 2024, 3 OSA and 3 control patients were recruited at the First Hospital of Hebei Medical University (Shijiazhuang, China). All patients were male, ranging in age from 42 to 57 years, with a median age of 49 years. Inclusion criteria for the control group: Healthy individuals matched with the age and sex of the study population and signed an informed consent form. Exclusion criteria: i) Those with serious comorbidities (for example, cardiovascular disease, severe hepatic or renal insufficiency); ii) patients who are using drugs that may affect the results of the study or have received related treatments; and iii) pregnant or breastfeeding women, or patients with psychiatric disorders who are unable to cooperate in the study. According to the diagnostic guidelines for patients with OSA (23)/hypopnoea syndrome (OSAHS), the inclusion criteria were as follows: i) Adults over the age of 18; ii) patients with symptoms of OSA, such as nocturnal snoring with apnea and daytime somnolence (24); and iii) examination showing upper airway stenosis and obstruction, with >30 recurrent apneas and hypopneas or a sleep apnea-hypopnea index (AHI) of ≥5 episodes/h during a 7-h sleep cycle per night. The exclusion criteria were as follows: i) Patients with pulmonary hypertension, bronchial asthma, chronic obstructive pulmonary disease and other pulmonary diseases and other sleep apnea disorders diagnosed before or during hospitalization; ii) patients with heart disease, chronic kidney disease, liver dysfunction or respiratory failure, mental disorders or other systemic illnesses; iii) patients who had taken or were taking medications affecting sleep and respiration within a short period before the consultation; iv) patients who have taken or are taking drugs that affect the sleep and respiratory system within a short period before the consultation; v) patients with upper respiratory tract infection within a short period before the consultation; vi) patients who did not agree to sign the informed consent form. In the present study, 10 ml whole blood samples from each of three patients with OSA and three normal controls were collected using anticoagulated blood tubes. The whole blood sample and phosphate buffer were mixed in a homogeneous 1:1 ratio (by adding 10 ml of phosphate buffer to 10 ml of whole blood sample and mixing). Subsequently, 10 ml of lymphocyte isolate (cat. no. 10771; Sigma-Aldrich; Merck KGaA) was added to each of six 50-ml centrifuge tubes, followed by the gentle addition of 20 ml of whole blood-phosphate mixture to the upper surface of the lymphocyte isolate. The tubes were then centrifuged for 30 min (447 x g; 20˚C). Finally, carefully the turbid layer at the junction of the middle and upper layers was collected and transfered to a new 50 ml centrifuge tube. Finally, the cloudy layer was washed three times with phosphate buffer, centrifuged repeatedly to precipitate the cells and the supernatant was discarded. This study was approved by the Ethics Committee of the First Hospital of Hebei Medical University (Shijiazhuang, China, approval number: 2024-082Y) in May 2024, and all subjects provided written informed consent to participate in the study. The study was conducted by the relevant guidelines and regulations.

Reverse transcription-quantitative PCR (RT-qPCR). Total RNA samples were extracted from the PBMCs using the Eastep® Super Total RNA Extraction Kit (Promega Shanghai Ltd.), which was used accordance with the manufacturer's instructions. The purity and concentration of total RNA were measured using a Nanodrop 1000 (Thermo Fisher Scientific, Inc.). Total RNA was reverse transcribed into cDNA using the GoScript™ Reverse Transcription kit (Promega Corporation) according to the manufacturer's protocol. qPCR was subsequently performed using the BlazeTaq™ SYBR® Green qPCR Mix 2.0 (GeneCopoeia) (Table I). The following thermocycling conditions were used for qPCR: 1 cycle at 95˚C for 30 sec, followed by 40 cycles of 10 sec at 95˚C, 20 sec at 60˚C and 30 sec at 72˚C. Relative mRNA levels were normalized to the level of GAPDH using the $2^{-\Delta\Delta Cq}$ method (25).

Table I. Sequences of primers for quantitative PCR.

Direction	Primer sequence (5'-3')
TXN	
Forward	AGACTCCAGCAGCCAAGATG
Reverse	GCAACATCATGAAAGAAAGGCT
EGR1	
Forward	CCCACCATGGACAACTACCC
Reverse	AAAGACTCTGCGGTCAGGTG
CDKN1A	
Forward	TGCCGAAGTCAGTTCCTTGT
Reverse	CATTAGCGCATCACAGTCGC
GAPDH	
Forward	GGAGCGAGATCCCTCCAAAAT
Reverse	GGCTGTTGTCATACTTCTCATGG

Statistical analysis. SPSS software version 26 (IBM Corp.) was used for statistical analysis. The data were tested for normality using the Shapiro-Wilk test and all data conformed to a normal distribution ($P>0.05$). Therefore, independent samples t-test was used to analyze the data. Data are expressed as mean ± SEM and the experiment was repeated at least 3 times. $P<0.05$ was considered a statistically significant difference.

Results

Screening for differential genes. Two datasets, GSE135917 and GSE38792, were merged into one. There was a batch effect between the different datasets (Fig. 2A) and the normalization eliminated the between-batch variations. The results are shown in the PCA plots before and after normalization (Fig. 2B). After data merging and processing, the genes were obtained after data correction and standardization. A total of 165 DEGs (Table SI) were identified between OSA and normal controls, and 114 upregulated genes and 51 downregulated genes were shown in the volcano plot and heatmap (Fig. 2C and D). KEGG pathway enrichment analysis was used to analyze DEGs. KEGG analysis showed that DEGs were enriched in the metabolic pathway (Fig. 3A; Table SII). The intersection of 484 ferroptosis-related genes and DEGs was taken to obtain OSA ferroptosis-related DEGs, totaling 10 genes (Fig. 3B; Table SIII). KEGG and GO analyses were performed on

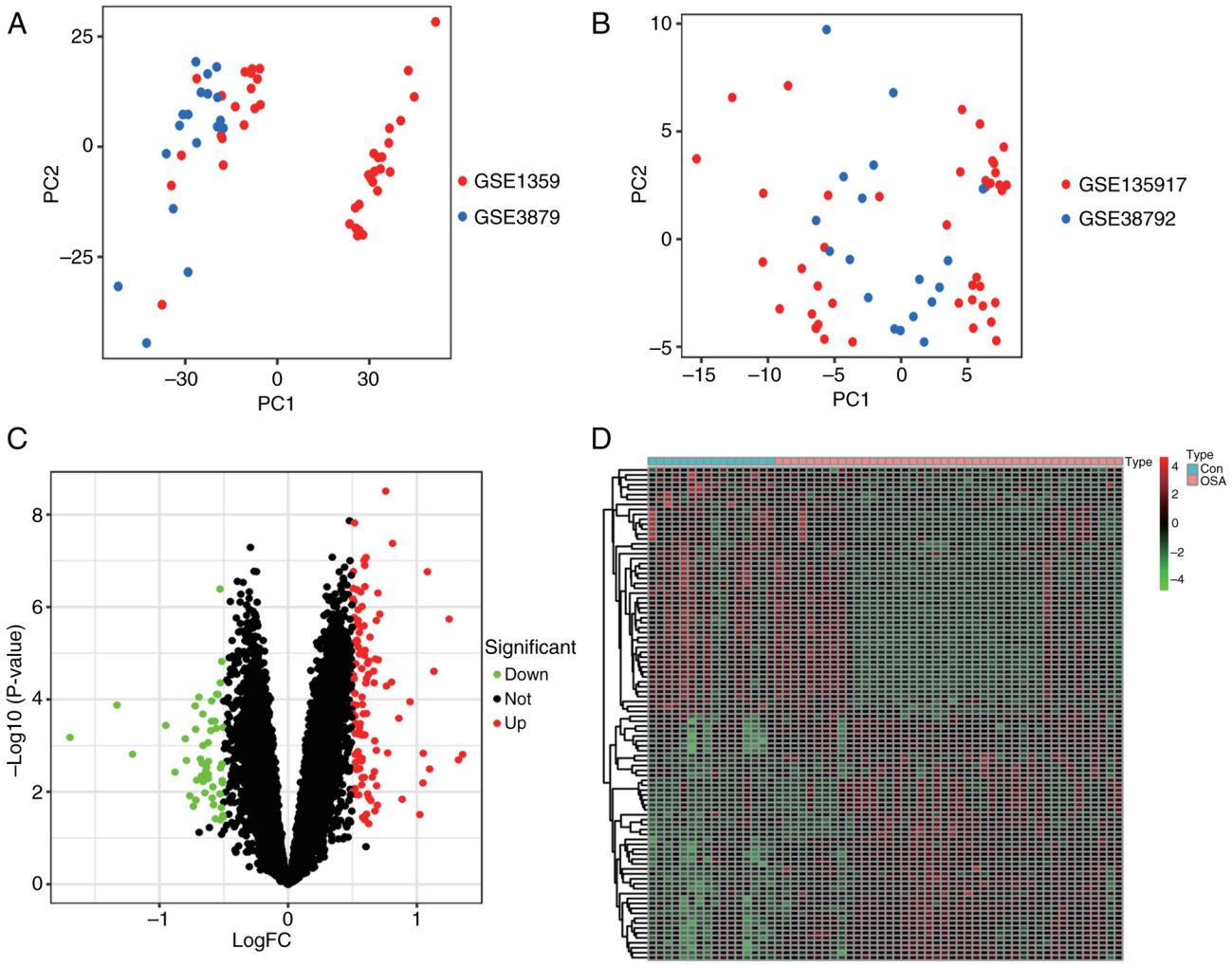

Figure 2. Screening for differential genes. (A and B) Two-dimensional PC analysis cluster plot of (A) GSE135917 and (B) GSE38792 samples before and after correction of the dataset. (C) The volcano plots of DEGs in the merged dataset (n=165, P<0.05). (D) Heatmap of DEGs in the merged dataset. PC, principal component; OSA, obstructive sleep apnea; con, control; FC, fold change; DEG, differentially expressed gene.

the intersecting DEGs, and GO analyses (Fig. 3D) revealed the involvement of a number of notable processes, such as 'regulation of smooth muscle cell proliferation' and 'regulation of smooth muscle cell proliferation'. Whereas the KEGG analysis (Fig. 3C; Table SIV) revealed processes mainly involved in immune infiltration, such as 'Human T-cell leukemia virus 1 infection' and 'Kaposi sarcoma-associated herpesvirus infection'.

Construction and module analysis of weighted gene co-expression network (WGCNA). WGCNA was used to identify clusters of co-expressed genes in OSA and to calculate the correlation between the combined modules and disease characterization. WGCNA analysis was performed using combined data from GSE135917 and GSE38792. Outliers were checked by sample clustering and no samples were removed from the combined data (Fig. S1). According to the approximate scale-free topology criterion, β=10 was chosen to determine the soft threshold in the OSA model (Fig. 4A and B). A hierarchical clustering tree was further developed, with each branch representing genes with similar expression and biological functions (Fig. 4C). After merging similar gene modules, four modules were identified in the OSA, as shown in Fig. 4D. Among the OSA modules, the grey module had the strongest positive correlation with OSA (r=0.49), and the turquoise module had the strongest negative correlation with the occurrence of OSA (r=-0.46) (Table SV).

Identification of shared genes and shared pathways. A total of nine genes overlapped in the strongest modules of OSA ferroptosis genes and WGCNA (Fig. 5A; Table SVI) Subsequently, GSEA analysis was performed on the OSA samples and it was found that the immune response was involved in common pathogenic processes (Fig. 5B).

Screening of feature genes. To narrow down the potential shared diagnostic gene biomarkers among the 9 DEGs, the LASSO (Fig. 6A and B) and RF (Fig. 6C and D) methods were used. With the help of LASSO regression and RF, 3 key genes were mined (Fig. 6E; Table SVII), namely TXN, EGR1 and CDKN1A.

Candidate biomarker expression levels and diagnostic value. The expression of the three key genes was identified in the merged dataset. Differential expression analysis showed that

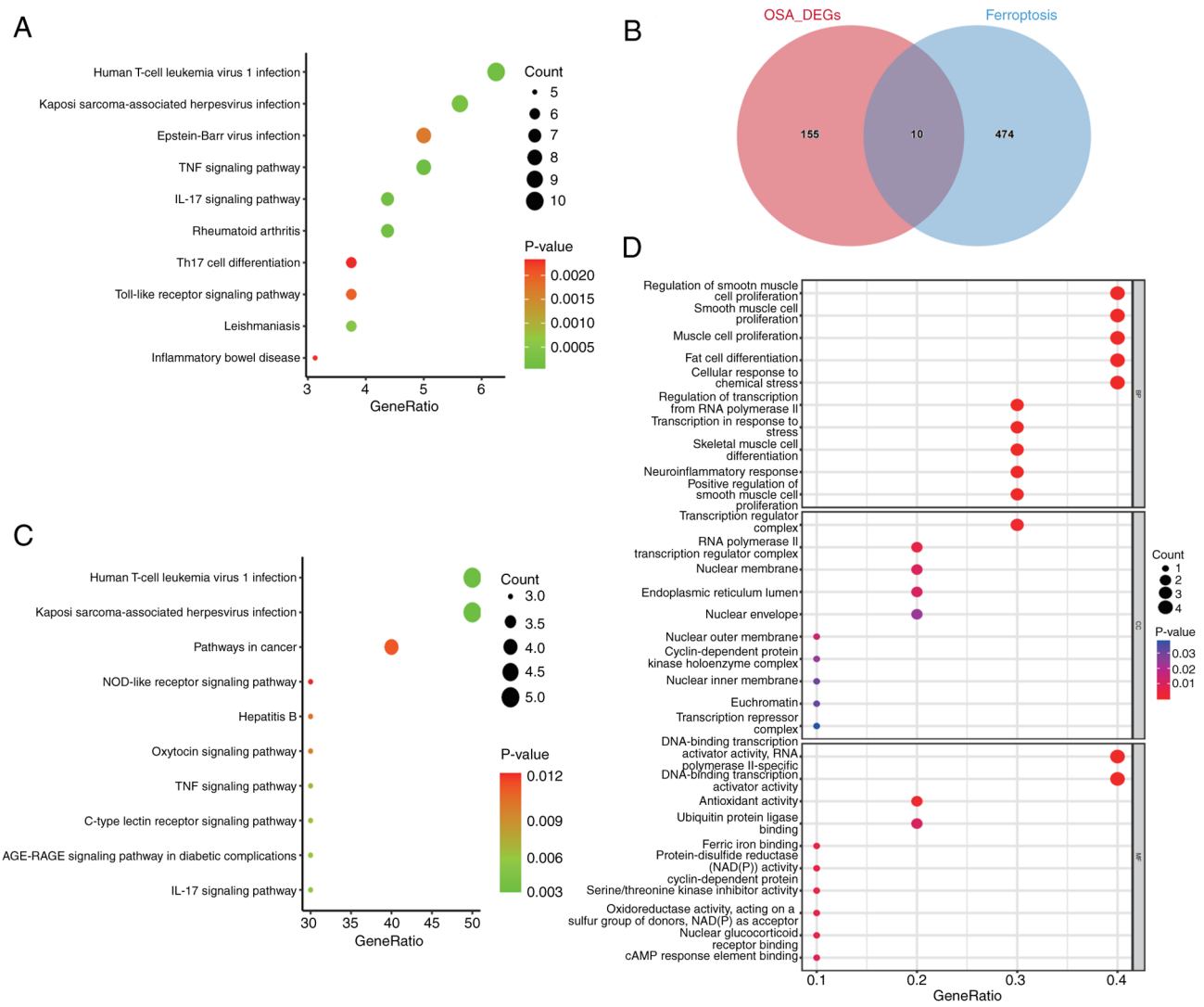

Figure 3. Differential genes enrichment analysis. (A) KEGG analysis of 165 genes in the OSA group compared to the control group. (B) Venn diagram of the intersection of 165 DEGs and ferroptosis-related genes. (C) KEGG analysis of 10 genes. (D) Gene Ontology analysis of 10 genes. OSA, obstructive sleep apnea; DEG, differentially expressed gene; MF, molecular function; BP, biological process; CC, cellular component; KEGG, Kyoto Encyclopedia of Genes and Genomes.

TXN was significantly highly expressed in OSA (Fig. 7A), and EGR1 and CDKN1A were significantly downregulated in OSA (Fig. 7B and C). The diagnostic ability of these three key markers was further determined based on ROC analysis, and the AUCs obtained for all three genes were >0.7 (Fig. 7D-F), showing relatively satisfactory diagnostic efficiency.

RT-qPCR. To verify the expression of the above key marker genes, fresh whole-blood samples were collected from 6 patients (3 OSA, 3 controls), PBMCs were extracted and RT-qPCR analysis was performed to verify the differential expression of TXN, EGR1 and CDKN1A in the patient samples. The results showed increased TXN expression (Fig. 8A), decreased EGR1 expression (Fig. 8B) and decreased CDKN1A expression (Fig. 8C) in patients with OSA compared with normal subjects, consistent with the above analysis.

Key marker genes are closely associated with various pathways related to ferroptosis in OSA. GSVA analysis was used to compare the activation pathways caused by the differential expression of each marker gene. The results indicated that elevated TXN transcript levels inhibited glucose metabolism, whereas previous studies have shown that TXN and linoleic and linolenic acid metabolism are closely related (26,27), and its overexpression may induce ferroptosis in OSA through linoleic and linolenic acid metabolism (Fig. 9A). Upregulation of EGR1 activates glucose metabolism, inhibits lipid metabolism, suppresses lipolytic processes leading to fat accumulation and also inhibits complement and clotting pathways (Fig. 9B). Low expression of CDKN1A is associated with complement and coagulation pathways, and low expression of this gene inhibits purine and glucose metabolism (Fig. 9C). In the high expression group of these genes, a series of OSA ferroptosis pathways relevant to pathogenesis was enriched.

Immune cell infiltration and its correlation with candidate biomarkers. Considering the important role of the immune response in the development of OSA, the differences in immune cell infiltration in the samples were further investigated. A total of 28 immune cell types were identified in the samples

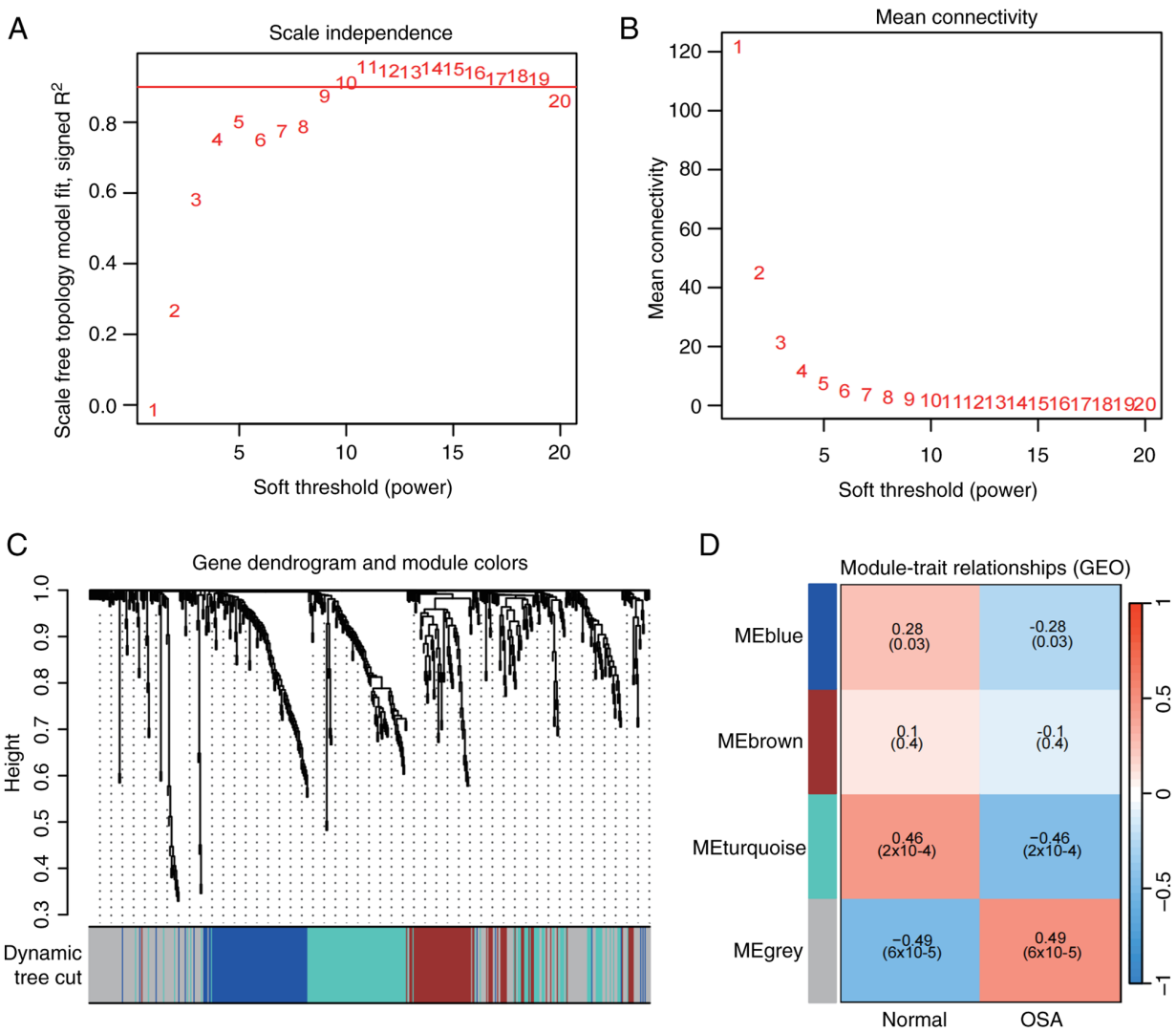

Figure 4. Construction and module analysis of weighted gene co-expression network. Analysis of the (A) scale-free index and (B) mean connectivity of various soft thresholds, with the red line indicating the selected soft threshold. (C) Cluster dendrogram of co-expression in OSA. (D) Correlation between modules and clinical traits in OSA. The numbers in the figure, as well as the (numbers), represent the correlation coefficients between the modules and the diseases, as well as the P-value, respectively. OSA, obstructive sleep apnea; ME, module eigengene; GEO, gene expression omnibus.

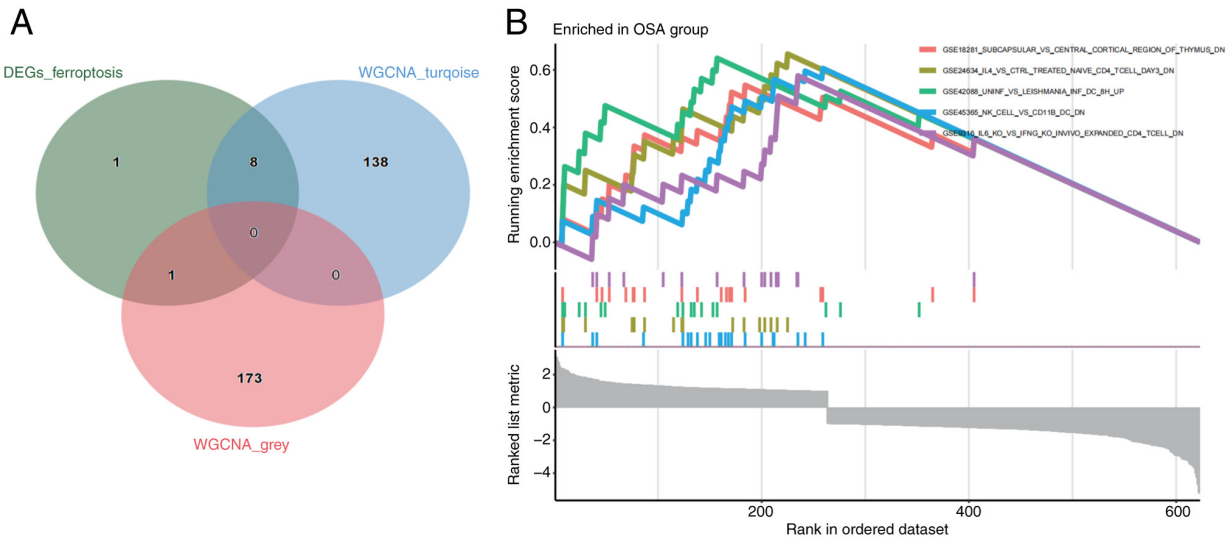

Figure 5. Identify shared genes and shared pathways. (A) Venn diagram showing the overlap of OSA ferroptosis-related genes and nine genes in the WGCNA module. (B) Results of single-gene gene set enrichment analysis of DEGs in OSA. OSA, obstructive sleep apnea; DEG, differentially expressed gene; WGCNA, weighted gene co-expression network.

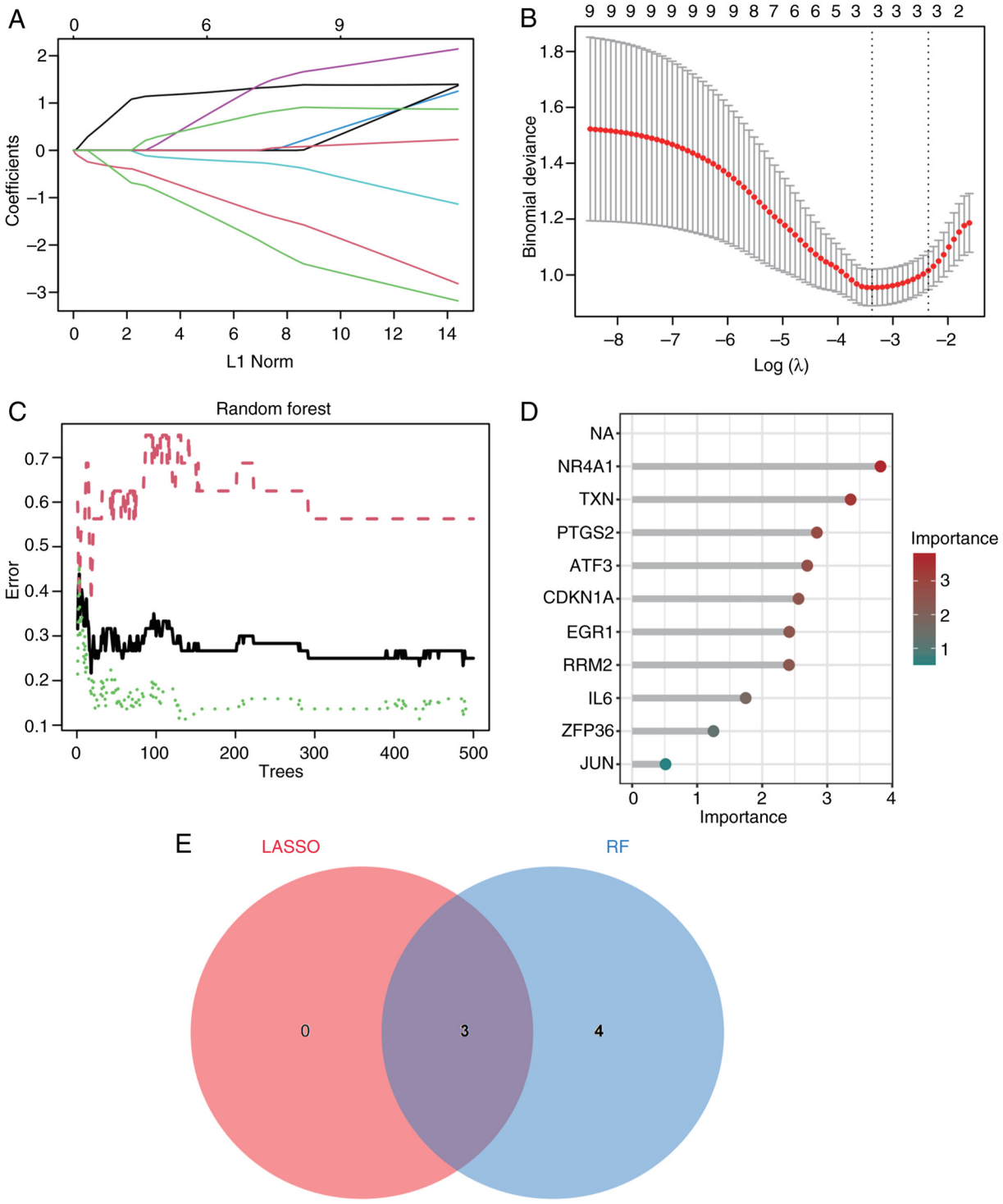

Figure 6. Screening feature genes. (A) LASSO coefficient profile of shared genes in the dataset. (B) Potentially shared diagnostic genes were identified using the LASSO regression model. A 10-time cross-validation was performed to select the optimal tuning parameter log (lambda). (C) The RF algorithm shows the error in average variable contribution; (D) The control group and genes are ranked based on the importance score. (E) Venn diagram of the intersection of genes screened by LASSO and RF. LASSO, the least absolute shrinkage and selection operators; RF, random forest.

and are shown in the heatmap and violin plot (Fig. 10A and B). Compared to the healthy controls, activated CD4 T cells, activated CD8 T cells, activated dendritic cells, CD56 bright natural killer (NK) cells, gamma delta T cells, immature dendritic cells, myeloid-derived suppressor cells, macrophages, mast cells, monocytes, NK T cells, NK cells, neutrophils, plasmacytoid dendritic cells, regulatory T cells, T follicular helper cells, type I T helper cells, effector memory CD4 T cells, central memory CD4 T cells and 17 other immune cell types were differentially infiltrated in patients with OSA and were upregulated in OSA tissues. In addition, the key biomarkers screened were closely associated with immune cells (Fig. 10C). In OSA samples, TXN expression was significantly correlated with type 17 T helper cells, plasmacytoid dendritic cells, mast cells, CD56 dim NK cells, activated dendritic cells and activated CD4 T cells; EGR1 expression was significantly correlated with mast cells,

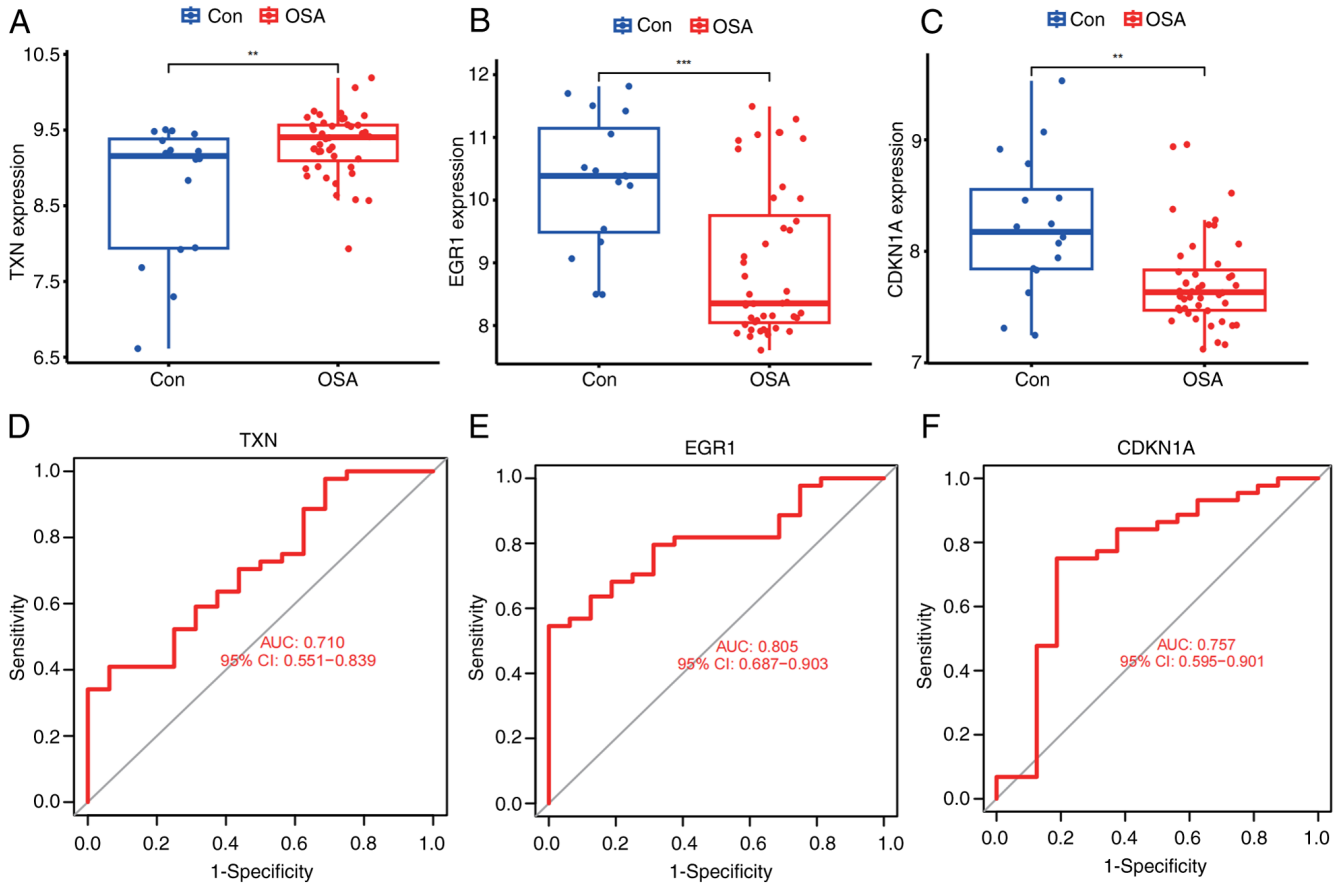

Figure 7. Candidate biomarker expression levels and diagnostic value. Validation and diagnostic value of expression of key biomarkers. (A) TXN, (B) EGR1 and (C) CDKN1A expression in the combined gene set. ROC curves for (D) TXN, (E) EGR1 and (F) CDKN1A in the combined gene set. **P<0.01; ***P<0.001. OSA, obstructive sleep apnea; Con, control; AUC, area under the ROC curve; ROC, receiver operating characteristic.

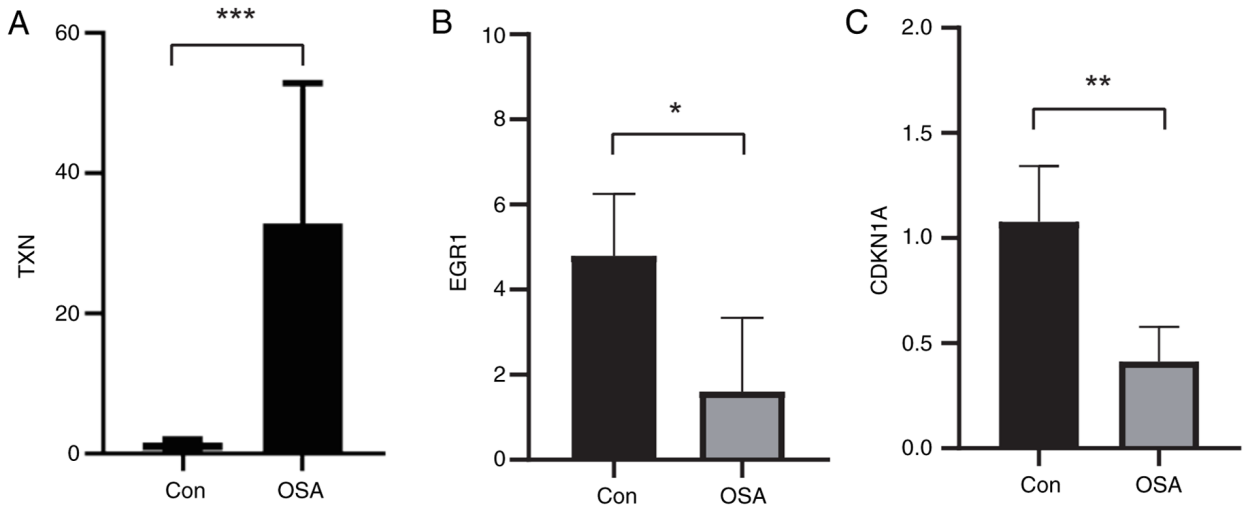

Figure 8. Expression levels of candidate biomarkers in patients with OSA. mRNA expression levels of (A) TXN, (B) EGR1 and (C) CDKN1A were determined by reverse transcription-quantitative PCR in peripheral blood mononuclear cells from patients and healthy controls. *P<0.05, **P<0.01; ***P<0.001. OSA, obstructive sleep apnea; Con, control.

eosinophils, effector memory CD8 T cells, central memory CD8 T cells, type 17 T helper cells, T follicular helper cells, plasmacytoid dendritic cells, NK T cells, NK cells and gamma delta T cells; and CDKN1A expression was significantly correlated with neutrophils, monocytes and eosinophils.

Prediction of key marker gene-targeted drugs. Through the DGIdb database, potential pharmacological targets were further identified. As a possible targeted drug, Genipin was identified for EGR1 (Interaction Score, 58.98; Fig. 11).

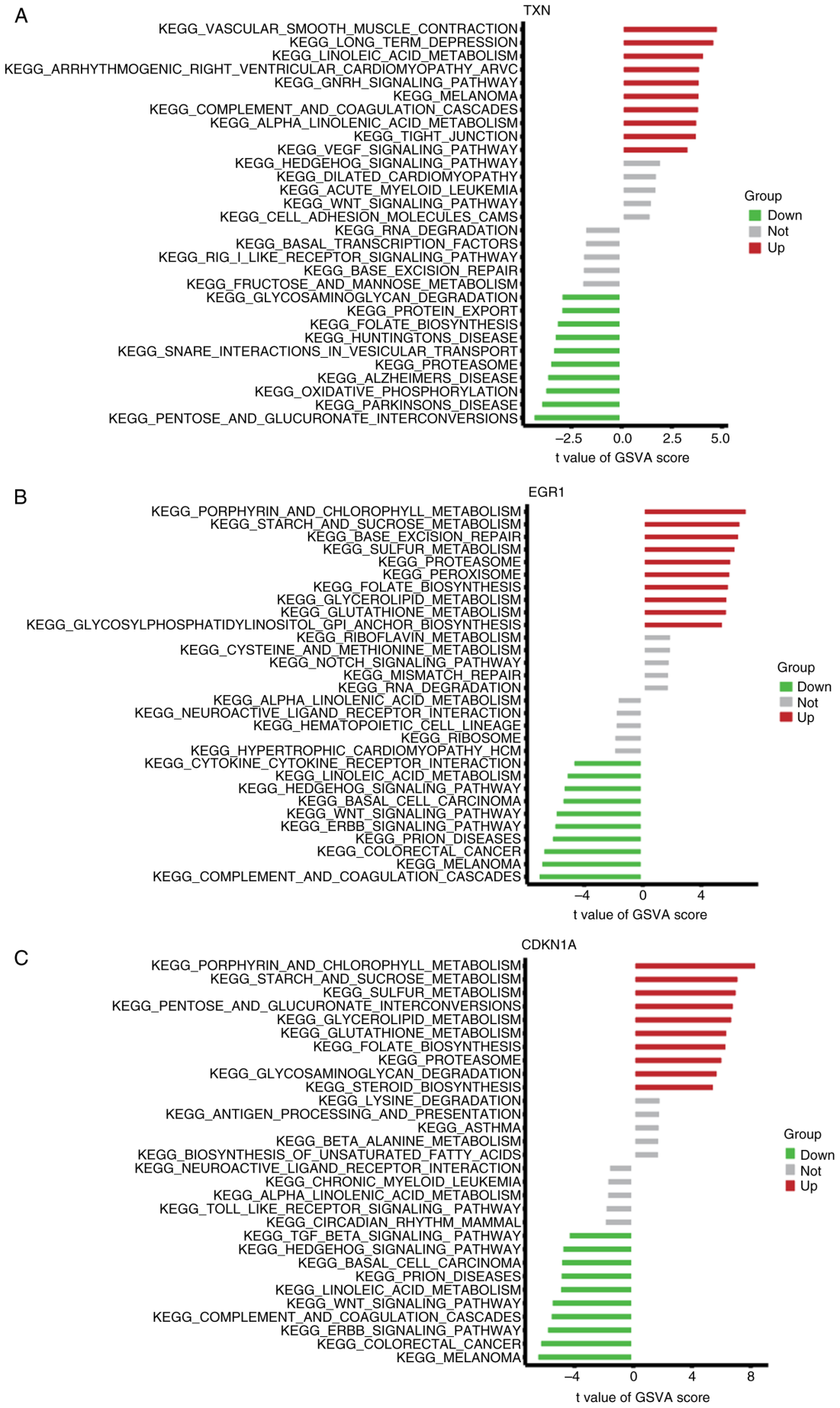

Figure 9. GSVA of three differential key marker genes. GSVA of (A) TXN, (B) EGR1 and (C) CDKN1A. GSVA, gene set variation analysis; KEGG, Kyoto Encyclopedia of Genes and Genomes.

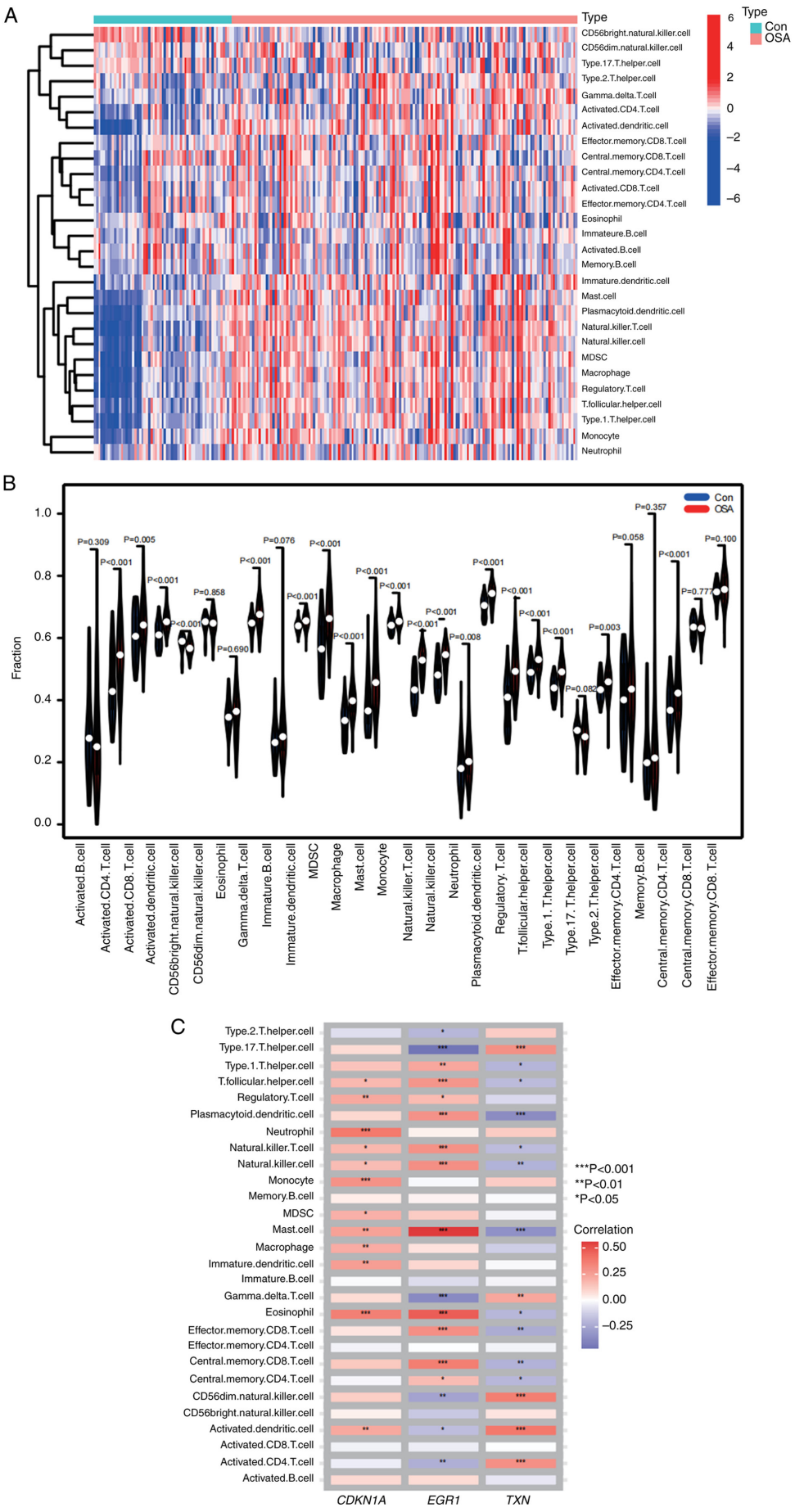

Figure 10. Analysis of immune infiltration associated with OSA. (A) Heatmap and (B) violin plot showing the distribution of 28 immune cells in merged datasets. (C) Association of key marker genes in samples with immune cell infiltration. *P<0.05, **P<0.01; ***P<0.001. OSA, obstructive sleep apnea; Con, control.

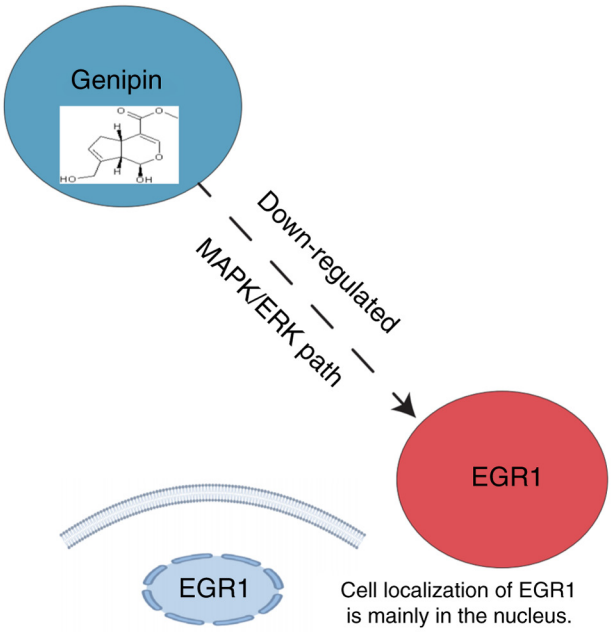

Figure 11. Targeted drugs based on the DGIdb database for the prediction of key differential marker genes.

CeRNA network based on marker genes. A ceRNA network was constructed based on three key marker genes using the miRanda, miRDB and TargetScan databases. The network consisted of 32 nodes (3 marker genes, 24 miRNAs and 5 lncRNAs). It was found that hsa-miR-12136, hsa-miR-196a-1-3p, hsa-miR-23a-3p, hsa-miR-23b-3p, hsa-miR-23c, hsa-miR-33a-3p and hsa-miR-3609 may competitively regulate TXN. Furthermore, lncRNA (RP11-333E1.2), which can control EGR1 expression through antagonistic binding to hsa-miR-125b-2-3p, was identified. In the CDKN1A ceRNA network, the lncRNAs of AC011718.2, RP11-94C24.13, LINC01106 and MUC19 could bind to hsa-let-7a-2-3p, hsa-let-7a-5p, hsa-miR-106a-5p and hsa-miR-1207-3p, respectively, to regulate genes (Fig. 12).

Discussion

Ferroptosis is a new hotspot of current research exploring new biomarkers and therapeutic targets, but research on OSA remains incomplete. In previous studies, chronic intermittent hypoxia was shown to generate large amounts of reactive oxygen species through repeated hypoxia-reoxygenation cycles, leading to lipid peroxidation (28), a central feature of ferroptosis. CIH may exacerbate lipid peroxidation by modulating iron metabolism-related proteins (e.g., transferrin receptor, ferritin) to increase intracellular free iron levels (13). CIH also imbalances the antioxidant system, leading to glutathione depletion or reduced glutathione peroxidase four activity, which impairs cellular scavenging of lipid peroxidation, thereby promoting ferroptosis (29). This suggests that OSA disease and ferroptosis mechanisms are closely related, and the search for key regulatory proteins related to ferroptosis in OSA is of high significance. Three key marker genes associated with ferroptosis in OSA were identified in the present study, which may enhance the understanding of the relationship between ferroptosis and OSA mechanisms. Furthermore, an immune infiltration analysis was performed to investigate new treatment programs for OSA, which may aid in the discovery of new therapeutic targets for OSA.

OSA is a disease whose onset and progression are not well established, and several previous studies have shown that the pathogenesis of OSA is closely related to hypoxia, oxidative stress and inflammation (30,31). In the current study, 114 upregulated and 51 downregulated genes were identified by merging and analyzing the data. KEGG pathway enrichment analysis showed that differentially expressed ferroptosis-related genes were mainly enriched in metabolic pathways and the PI3K/Akt pathway, while it was found that the immune pathway was the major enriched pathway for ferroptosis-related genes in OSA.

OSA is strongly associated with metabolic disorders and the prevalence of OSA is high in diabetic patients, ranging between 17 and 48% (32). CIH is a key pathophysiologic feature of OSA and can cause most of the pathological changes modeled in OSA. Previous studies have shown that CIH interferes with glucose metabolism by affecting insulin secretion and directly affecting pancreatic islet organs (33,34), and that insulin sensitivity is decreased in adipocytes exposed to CIH conditions (35,36). It has also been shown that OSA-induced hypoxia increases metabolites such as lactate and certain fatty acids in the blood (37,38). Similarly, sleep plays an important role in regulating endocrine function and glucose metabolism, and poor sleep quality and short sleep duration may contribute to glucose metabolism disorders in patients with OSA, which can increase the risk of diabetes (39). In addition, OSA is an independent risk factor for insulin resistance and fatty liver, may trigger metabolic mitochondrial energy-related processes, and can also induce inflammation and lead to dysfunction in adipose tissue, while altering lipid metabolism and obesity (40,41). An interesting point was found in the GSVA analysis performed in the present study, namely that TXN may induce ferroptosis in OSA through linoleic and linolenic acid metabolism. Previous studies have found that TXN may antagonize the lipogenesis of peroxisome proliferator-activated receptor (PPAR)γ *in vivo*, and PPARγ plays a key role in fatty acid metabolism, which may be related to the metabolism of linoleic acid and linolenic acid. It has been found that TXN may regulate linolenic acid metabolism and its physiological functions by affecting signaling pathways such as MAPK and PI3K/Akt (27). By contrast, lipid peroxides from linoleic acid metabolism can drive ferroptosis (42,43). Among them, linoleic acid-rich phospholipids (e.g., phosphatidylethanolamine) in cell membranes are key targets of ferroptosis and their oxidation leads to disruption of membrane integrity (44). Disorders of linoleic acid metabolism may also be associated with ferroptosis-related metabolic disorders (e.g., nonalcoholic fatty liver disease) and neuronal ferroptosis in neurodegenerative diseases (e.g., Alzheimer's disease, Parkinson's disease) (45).

The present enrichment analysis of the differential genes revealed a close relationship between OSA and the immune response, and several studies have shown that an important pathological feature of OSA is immune cell infiltration (46). Therefore, an immune cell infiltration analysis was performed to understand the role of these immune cells in OSA. The results suggest that T lymphocytes are

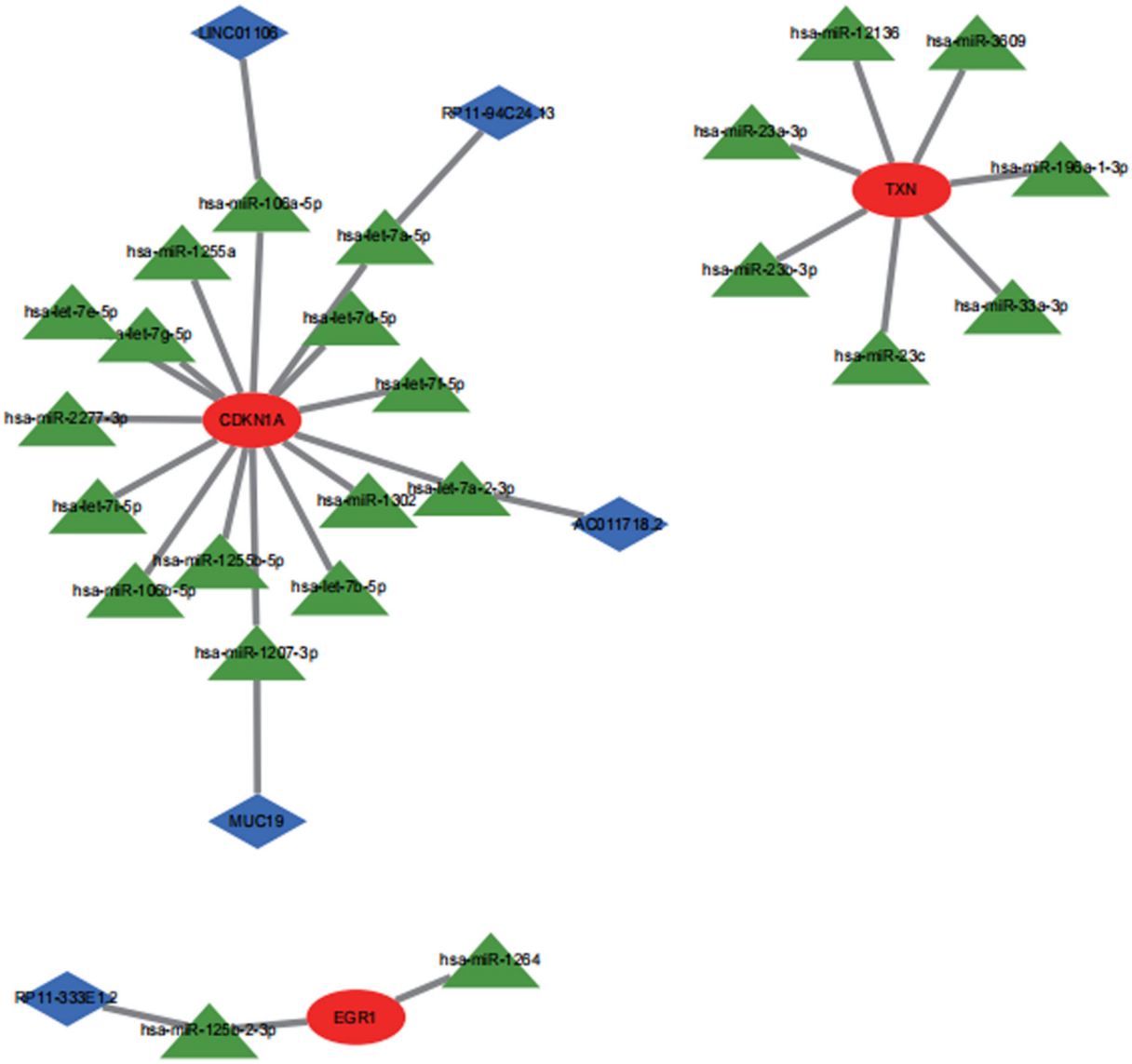

Figure 12. Competing endogenous RNA networks of TXN, EGR1, CDKN1A and the potential RNA regulatory pathways. miR, microRNA.

the main cells enriched in OSA; T lymphocytes are present in peripheral blood and tissue fluids and perform cellular immunity and immunomodulatory functions, and OSA may be associated with changes in T-cell levels, activation and proliferation. In the study of cellular immune response in OSA by Dyugovskaya *et al* (47), cellular immune response plays an important role in the progression of the disease course of OSA. Cell counts of CD4 and CD8 T cells were significantly increased in patients with OSA compared with normal controls (48), and T-lymphocytes showed high expression of activation and cytotoxicity. Furthermore, Another study reported that effector CD4 T cells were upregulated in children with a high AHI (49). Also, CD4 and CD8 T cells isolated from the tonsils of children with OSA had an increased ability to proliferate *in vitro* (50). In addition, in OSA, lymphocyte B, NK and NKT-like cells are equally involved in its pathology and play a stronger role in its complications (51). Atherosclerosis is a known common complication of OSA and NKT cells have been shown to contribute to the development of atherosclerosis in OSA, so there may be a role for NKT cells in atherosclerosis caused by OSA.

In this study, the key genes screened by LASSO and the key genes screened by RF were intersected, and three common key marker genes TXN, EGR1 and CDKN1A were obtained. Their ROC curves were plotted separately and the AUC values of these three genes were all >0.7, indicating that they have a certain diagnostic significance. TXN, EGR1 and CDKN1A may be biological markers of ferroptosis in OSA. At the same time, the present GSVA analysis of the 3 key genes showed that metabolic pathways, including sugar and lipid metabolism, were likewise mainly involved between groups with high and low gene expression levels.

TXN is one of the most common markers of oxidative stress, which is a typical feature of OSA. Previous studies have shown that the degree of TXN expression represents the severity of OSA (52) and may be useful in evaluating and monitoring patients with OSA (53). TXN is also used in the clinic to monitor the efficacy of transnasal continuous positive airway pressure in the treatment of OSA (54). TXN

levels were upregulated in patients with OSA in the present study and may represent the oxidative stress process involved in OSA. EGR1 was also reported to be involved in oxidative stress and can lead to cardiac hypertrophy (55,56). In addition, previous studies have shown that EGR1 inhibits adipose triglyceride lipase to inhibit lipolysis, which leads to fat accumulation (57) and promotes adipocyte differentiation and activation (58). The present results showed decreased EGR1 expression in patients with OSA, which may imply increased lipolysis and disturbed lipid metabolism. CDKN1A, also known as p21 or WAF1, is one of the key molecules in cell cycle regulation. It is involved in cell cycle arrest, DNA damage repair, cellular senescence and apoptosis by inhibiting the activity of CDKs (59). Previous studies have shown that downregulating CDKN1A leads to decreased cellular repair of DNA damage and increased genomic instability (60). In the present results, CDKN1A expression was downregulated in patients with OSA, which may represent a decreased ability to repair DNA damage in OSA disease.

In addition, potential pharmacological targets were identified through the DGIdb database and a possible target drug, Genipin, was discovered for EGR1. Genipin has a wide range of biological activities, including protein regulation, anti-tumor, anti-inflammatory, immunosuppressive and anti-thrombotic (61). EGR1 is an important nuclear transcription factor involved in regulating the cell growth and differentiation process, modulating the expression of immune-related genes and influencing the inflammatory response and the function of immune cells (62). A previous study has shown that EGR1 is a key target for Genipin (63). In the present study, it was found that EGR1 is a key gene associated with ferroptosis in OSA, and there was a statistically significant difference in the expression of EGR1 between OSA and controls. EGR1 may be a target for early diagnosis and treatment of OSA, and it may be possible to ameliorate disease damage in OSA by targeting EGR1 with Genipin. However, at the same time, Genipin also has certain potential side effects (64), such as a certain degree of cytotoxicity, affecting cell viability and proliferation, and it can cause excessive immune responses. Therefore, it is still necessary to explore the potential avenues for the safe treatment of OSA with Genipin in the future.

In addition, the ceRNA network centered on key marker genes was mapped in the present study. LncRNAs regulate the expression of 3 key marker genes by competing with mRNAs to bind miRNAs. Wu *et al* (15) proposed an lncRNA-miRNA-mRNA ceRNA network to help explore the molecular mechanisms of lung adenocarcinoma. Wang *et al* (65) treated osteoarthritis by identifying key lncRNAs. The results of the present study suggested that the combination of hsa-miR-12136, hsa-miR-196a-1-3p, hsa-miR-23a-3p, hsa-miR-23b-3p, hsa-miR-23c, hsa-miR-33a-3p and hsa-miR-3609 may competitively regulate TXN. An lncRNA can control EGR1 expression through antagonistic binding to hsa-miR-125b-2-3p. In the CDKN1A ceRNA network, four lncRNAs can respectively bind to hsa-let-7a-2-3p, hsa-let-7a-5p, hsa-miR-106a-5p and hsa-miR-1207-3p to regulate genes. This suggests that these miRNAs, which directly regulate mRNAs, and lncRNAs, which indirectly regulate the expression of mRNAs, may also be possible targets for the prevention and treatment of OSA and have the potential to be therapeutic targets for OSA.

There are certain limitations to the present study. First, only data retrieved from the GEO database were included, which is an insufficient sample size. Furthermore, due to the small number of datasets available for OSA, the present analysis was not validated by any external datasets, which may lead to one-sided results. The present findings need to be validated in a larger sample. More importantly, the current study lacks valid experimental data to confirm the actual therapeutic effect between the discovered drugs and OSA. Finally, more studies on the specific associations between lncRNAs and miRNAs with key genes are also needed. Therefore, it is planned to expand the sample size for further validation and prepare experiments in our group to confirm the therapeutic effects of the identified drugs.

In conclusion, in the present study, three key differential genes, TXN, EGR1 and CDKN1A, were screened, which may serve as potential biomarkers of ferroptosis in OSA. The possible mechanisms of action of three key marker genes in OSA were explored in a bioinformatics analysis. The results regarding the newly discovered EGR1-targeting drug Genipin and the related lncRNAs found in the ceRNA network constructed may provide new ideas for the targeted treatment of OSA. In this paper, ferroptosis-related genes in OSA were explored and their potential clinical value was discussed to provide potential diagnostic and therapeutic targets for OSA. These results provide a reference for further research on the therapeutic mechanisms of OSA and the development of targets for drug intervention. In future studies, the sample size will be expanded and *in vivo* and *in vitro* experiments will be combined to further investigate the reliability of the screened biomarkers as diagnostic and therapeutic targets for OSA and to characterize the therapeutic efficacy of related drugs.

Acknowledgements

Not applicable.

Funding

This research was funded by the Hebei Province Natural Science Foundation of China (grant no. H2023206407) and the Training Program Foundation for the Talents of Clinical Medicine sponsored by the Chinese Government (grant no. ZF2024128).

Availability of data and materials

The data generated in the present study may be requested from the corresponding author.

Authors' contributions

BC contributed to the conception and design. BC and LD analyzed the data. WC validated the method and data. BC wrote the manuscript. DS edited the manuscript and provided constructive comments. All authors read and approved the final manuscript. BC and DS confirm the authenticity of the raw data.

Ethics approval and consent to participate

This study was conducted in accordance with the guidelines of the Declaration of Helsinki and was approved by the Ethics Committee of the First Hospital of Hebei Medical University (Shijiazhuang, China; approval no. 2024-082Y). The written informed consent includes a description of the study, the rights of the participants, and the storage and release of their data for the purpose of participating in the study; all patients (including the control group) provided written informed consent.

Patient consent for publication

Not applicable.

Competing interests

The authors declare that they have no competing interests.

References

1. Hou H, Zhao Y, Yu W, Dong H, Xue X, Ding J, Xing W and Wang W: Association of obstructive sleep apnea with hypertension: A systematic review and meta-analysis. J Glob Health 8: 010405, 2018.
2. Lebkuchen A, Carvalho VM, Venturini G, Salgueiro JS, Freitas LS, Dellavance A, Martins FC, Lorenzi-Filho G, Cardozo KHM and Drager LF: Metabolomic and lipidomic profile in men with obstructive sleep apnoea: Implications for diagnosis and biomarkers of cardiovascular risk. Sci Rep 8: 11270, 2018.
3. Tripathi A, Melnik AV, Xue J, Poulsen O, Meehan MJ, Humphrey G, Jiang L, Ackermann G, McDonald D, Zhou D, *et al*: Intermittent hypoxia and hypercapnia, a hallmark of obstructive sleep apnea, alters the gut microbiome and metabolome. mSystems 3: e00020-18, 2018.
4. Chiu HY, Chou KT, Su KC, Lin FC, Liu YY, Shiao TH and Chen YM: Obstructive sleep apnea in young Asian adults with sleep-related complaints. Sci Rep 12: 20582, 2022.
5. Heinzer R, Vat S, Marques-Vidal P, Marti-Soler H, Andries D, Tobback N, Mooser V, Preisig M, Malhotra A, Waeber G, *et al*: Prevalence of sleep-disordered breathing in the general population: The HypnoLaus study. Lancet Respir Med 3: 310-318, 2015.
6. Benjafield AV, Ayas NT, Eastwood PR, Heinzer R, Ip MSM, Morrell MJ, Nunez CM, Patel SR, Penzel T, Pépin JL, *et al*: Estimation of the global prevalence and burden of obstructive sleep apnoea: A literature-based analysis. Lancet Respir Med 7: 687-698, 2019.
7. Dixon SJ, Lemberg KM, Lamprecht MR, Skouta R, Zaitsev EM, Gleason CE, Patel DN, Bauer AJ, Cantley AM, Yang WS, *et al*: Ferroptosis: An iron-dependent form of nonapoptotic cell death. Cell 149: 1060-1072, 2012.
8. Tang D, Kang R, Berghe TV, Vandenabeele P and Kroemer G: The molecular machinery of regulated cell death. Cell Res 29: 347-364, 2019.
9. Zhang JJ, Du J, Kong N, Zhang GY, Liu MZ and Liu C: Mechanisms and pharmacological applications of ferroptosis: A narrative review. Ann Transl Med 9: 1503, 2021.
10. He P, Xu S, Miao Z, Que Y, Chen Y, Li S, Ma Q, Yang R, Wei W, Zha Z and Hu Y: Anti-Her2 affibody-decorated arsenene nanosheets induce ferroptosis through depleting intracellular GSH to overcome cisplatin resistance. J Nanobiotechnology 21: 203, 2023.
11. Huang J, Xie H, Yang Y, Chen L, Lin T, Wang B and Lin QC: The role of ferroptosis and endoplasmic reticulum stress in intermittent hypoxia-induced myocardial injury. Sleep Breath 27: 1005-1011, 2023.
12. Zhang L, Guo Y, Xiaokereti J, Cao G, Li H, Sun H, Li K, Zhou X and Tang B: Ganglionated plexi ablation suppresses chronic obstructive sleep apnea-related atrial fibrillation by inhibiting cardiac autonomic hyperactivation. Front Physiol 12: 640295, 2021.
13. Liu ZL, Huang YP, Wang X, He YX, Li J and Li B: The role of ferroptosis in chronic intermittent hypoxia-induced cognitive impairment. Sleep Breath 27: 1725-1732, 2023.
14. Uesaka K, Oka H, Kato R, Kanie K, Kojima T, Tsugawa H, Toda Y and Horinouchi T: Bioinformatics in bioscience and bioengineering: Recent advances, applications, and perspectives. J Biosci Bioeng 134: 363-373, 2022.
15. Wu X, Sui Z, Zhang H, Wang Y and Yu Z: Integrated analysis of lncRNA-mediated ceRNA network in lung adenocarcinoma. Front Oncol 10: 554759, 2020.
16. Friedman J, Hastie T and Tibshirani R: Regularization paths for generalized linear models via coordinate descent. J Stat Softw 33: 1-22, 2010.
17. Dall'Alba G, Casa PL, Abreu FP, Notari DL and de Avila E Silva S: A survey of biological data in a big data perspective. Big Data 10: 279-297, 2022.
18. Dey D, Haque MS, Islam MM, Aishi UI, Shammy SS, Mayen MSA, Noor STA and Uddin MJ: The proper application of logistic regression model in complex survey data: A systematic review. BMC Med Res Methodol 25: 15, 2025.
19. Ma X, Han X and Zhang L: An improved k-nearest neighbor algorithm for recognition and classification of thyroid nodules. J Ultrasound Med 43: 1025-1036, 2024.
20. Ellis K, Kerr J, Godbole S, Lanckriet G, Wing D and Marshall S: A random forest classifier for the prediction of energy expenditure and type of physical activity from wrist and hip accelerometers. Physiol Meas 35: 2191-2203, 2014.
21. Zhang M, Zhu K, Pu H, Wang Z, Zhao H, Zhang J and Wang Y: An immune-related signature predicts survival in patients with lung adenocarcinoma. Front Oncol 9: 1314, 2019.
22. Alderden J, Pepper GA, Wilson A, Whitney JD, Richardson S, Butcher R, Jo Y and Cummins MR: Predicting pressure injury in critical care patients: A machine-learning model. Am J Crit Care 27: 461-468, 2018.
23. Epstein LJ, Kristo D, Strollo PJ Jr, Friedman N, Malhotra A, Patil SP, Ramar K, Rogers R, Schwab RJ, Weaver EM, *et al*: Clinical guideline for the evaluation, management and long-term care of obstructive sleep apnea in adults. J Clin Sleep Med 5: 263-276, 2009.
24. Kapur VK, Auckley DH, Chowdhuri S, Kuhlmann DC, Mehra R, Ramar K and Harrod CG: Clinical practice guideline for diagnostic testing for adult obstructive sleep apnea: An American academy of sleep medicine clinical practice guideline. J Clin Sleep Med 13: 479-504, 2017.
25. Livak KJ and Schmittgen TD: Analysis of relative gene expression data using real-time quantitative PCR and the 2(-Delta Delta C(T)) method. Methods 25: 402-408, 2001.
26. Zhang Y, Bobe G, Miranda CL, Lowry MB, Hsu VL, Lohr CV, Wong CP, Jump DB, Robinson MM, Sharpton TJ, *et al*: Tetrahydroxanthohumol, a xanthohumol derivative, attenuates high-fat diet-induced hepatic steatosis by antagonizing PPARγ. Elife 10: e66398, 2021.
27. Ibeagha-Awemu EM, Li R, Ammah AA, Dudemaine PL, Bissonnette N, Benchaar C and Zhao X: Transcriptome adaptation of the bovine mammary gland to diets rich in unsaturated fatty acids shows greater impact of linseed oil over safflower oil on gene expression and metabolic pathways. BMC Genomics 17: 104, 2016.
28. Prabhakar NR, Kumar GK, Nanduri J and Semenza GL: ROS signaling in systemic and cellular responses to chronic intermittent hypoxia. Antioxid Redox Signal 9: 1397-1403, 2007.
29. Chen LD, Wu RH, Huang YZ, Chen MX, Zeng AM, Zhuo GF, Xu FS, Liao R and Lin QC: The role of ferroptosis in chronic intermittent hypoxia-induced liver injury in rats. Sleep Breath 24: 1767-1773, 2020.
30. Singh JA and Cleveland JD: Gout and the risk of incident obstructive sleep apnea in adults 65 years or older: An observational study. J Clin Sleep Med 14: 1521-1527, 2018.
31. Wong MYZ, Yap JJL, Sultana R, Cheah M, Goh GBB and Yeo KK: Association between non-alcoholic fatty liver disease and subclinical atherosclerosis in Western and Asian cohorts: An updated meta-analysis. Open Heart 8: e001850, 2021.
32. Fallahi A, Jamil DI, Karimi EB, Baghi V and Gheshlagh RG: Prevalence of obstructive sleep apnea in patients with type 2 diabetes: A systematic review and meta-analysis. Diabetes Metab Syndr 13: 2463-2468, 2019.
33. Gozal D, Gileles-Hillel A, Cortese R, Li Y, Almendros I, Qiao Z, Khalyfa AA, Andrade J and Khalyfa A: Visceral white adipose tissue after chronic intermittent and sustained hypoxia in mice. Am J Respir Cell Mol Biol 56: 477-487, 2017.

34. Ryan S: Adipose tissue inflammation by intermittent hypoxia: Mechanistic link between obstructive sleep apnoea and metabolic dysfunction. J Physiol 595: 2423-2430, 2017.
35. Hirotsu C, Haba-Rubio J, Togeiro SM, Marques-Vidal P, Drager LF, Vollenweider P, Waeber G, Bittencourt L, Tufik S and Heinzer R: Obstructive sleep apnoea as a risk factor for incident metabolic syndrome: A joined Episono and HypnoLaus prospective cohorts study. Eur Respir J 52: 1801150, 2018.
36. Murphy AM, Thomas A, Crinion SJ, Kent BD, Tambuwala MM, Fabre A, Pepin JL, Roche HM, Arnaud C and Ryan S: Intermittent hypoxia in obstructive sleep apnoea mediates insulin resistance through adipose tissue inflammation. Eur Respir J 49: 1601731, 2017.
37. Papandreou C: Independent associations between fatty acids and sleep quality among obese patients with obstructive sleep apnoea syndrome. J Sleep Res 22: 569-572, 2013.
38. Xu H, Zheng X, Qian Y, Guan J, Yi H, Zou J, Wang Y, Meng L, Zhao A, Yin S and Jia W: Metabolomics profiling for obstructive sleep apnea and simple snorers. Sci Rep 6: 30958, 2016.
39. Tasali E, Leproult R and Spiegel K: Reduced sleep duration or quality: Relationships with insulin resistance and type 2 diabetes. Prog Cardiovasc Dis 51: 381-391, 2009.
40. Ryan S, Arnaud C, Fitzpatrick SF, Gaucher J, Tamisier R and Pépin JL: Adipose tissue as a key player in obstructive sleep apnoea. Eur Respir Rev 28: 190006, 2019.
41. Arısoy A, Sertoğullarından B, Ekin S, Özgökçe M, Bulut MD, Huyut MT, Ölmez Ş and Turan M: Sleep apnea and fatty liver are coupled via energy metabolism. Med Sci Monit 22: 908-913, 2016.
42. Beatty A, Singh T, Tyurina YY, Tyurin VA, Samovich S, Nicolas E, Maslar K, Zhou Y, Cai KQ, Tan Y, *et al*: Ferroptotic cell death triggered by conjugated linolenic acids is mediated by ACSL1. Nat Commun 12: 2244, 2021.
43. Sarparast M, Pourmand E, Hinman J, Vonarx D, Reason T, Zhang F, Paithankar S, Chen B, Borhan B, Watts JL, *et al*: Dihydroxy-metabolites of dihomo-γ-linolenic acid drive ferroptosis-mediated neurodegeneration. ACS Cent Sci 9: 870-882, 2023.
44. Perez MA, Clostio AJ, Houston IR, Ruiz J, Magtanong L, Dixon SJ and Watts JL: Ether lipid deficiency disrupts lipid homeostasis leading to ferroptosis sensitivity. PLoS Genet 18: e1010436, 2022.
45. Sarparast M, Pourmand E, Hinman J, Vonarx D, Reason T, Zhang F, Paithankar S, Chen B, Borhan B, Watts JL, *et al*: Dihydroxy-metabolites of dihomo-gamma-linolenic acid drive ferroptosis-Mediated Neurodegeneration. bioRxiv [Preprint]: 2023.01.05.522933, 2023.
46. Jelic S, Lederer DJ, Adams T, Padeletti M, Colombo PC, Factor PH and Le Jemtel TH: Vascular inflammation in obesity and sleep apnea. Circulation 121: 1014-1021, 2010.
47. Dyugovskaya L, Lavie P, Hirsh M and Lavie L: Activated CD8+ T-lymphocytes in obstructive sleep apnoea. Eur Respir J 25: 820-628, 2005.
48. Sériès F, Chakir J and Boivin D: Influence of weight and sleep apnea status on immunologic and structural features of the uvula. Am J Respir Crit Care Med 170: 1114-1119, 2004.
49. Sade K, Fishman G, Kivity S, DeRowe A and Langier S: Expression of Th17 and Treg lymphocyte subsets in hypertrophied adenoids of children and its clinical significance. Immunol Invest 40: 657-666, 2011.
50. Kim J, Bhattacharjee R, Dayyat E, Snow AB, Kheirandish-Gozal L, Goldman JL, Li RC, Serpero LD, Clair HB and Gozal D: Increased cellular proliferation and inflammatory cytokines in tonsils derived from children with obstructive sleep apnea. Pediatr Res 66: 423-428, 2009.
51. Domagała-Kulawik J, Osińska I, Piechuta A, Bielicki P and Skirecki T: T, B, and NKT cells in systemic inflammation in obstructive sleep apnoea. Mediators Inflamm 2015: 161579, 2015.
52. Guo Q, Wang Y, Li QY, Li M and Wan HY: Levels of thioredoxin are related to the severity of obstructive sleep apnea: Based on oxidative stress concept. Sleep Breath 17: 311-316, 2013.
53. Lira AB and de Sousa Rodrigues CF: Evaluation of oxidative stress markers in obstructive sleep apnea syndrome and additional antioxidant therapy: A review article. Sleep Breath 20: 1155-1160, 2016.
54. Takahashi K, Chin K, Nakamura H, Morita S, Sumi K, Oga T, Matsumoto H, Niimi A, Fukuhara S, Yodoi J and Mishima M: Plasma thioredoxin, a novel oxidative stress marker, in patients with obstructive sleep apnea before and after nasal continuous positive airway pressure. Antioxid Redox Signal 10: 715-726, 2008.
55. Xie B, Wang C, Zheng Z, Song B, Ma C, Thiel G and Li M: Egr-1 transactivates Bim gene expression to promote neuronal apoptosis. J Neurosci 31: 5032-5044, 2011.
56. Luo S, Garcia-Arencibia M, Zhao R, Puri C, Toh PP, Sadiq O and Rubinsztein DC: Bim inhibits autophagy by recruiting Beclin 1 to microtubules. Mol Cell 47: 359-370, 2012.
57. Singh M, Shin YK, Yang X, Zehr B, Chakrabarti P and Kandror KV: 4E-BPs control fat storage by regulating the expression of Egr1 and ATGL. J Biol Chem 290: 17331-17338, 2015.
58. Blé her M, Meshko B, Cacciapuoti I, Gergondey R, Kovacs Y, Duprez D, L'Honoré A and Havis E: Egr1 loss-of-function promotes beige adipocyte differentiation and activation specifically in inguinal subcutaneous white adipose tissue. Sci Rep 10: 15842, 2020.
59. Manousakis E, Miralles CM, Esquerda MG and Wright RHG: CDKN1A/p21 in breast cancer: Part of the problem, or part of the solution? Int J Mol Sci 24: 17488, 2023.
60. Perucca P, Cazzalini O, Madine M, Savio M, Laskey RA, Vannini V, Prosperi E and Stivala LA: Loss of p21 CDKN1A impairs entry to quiescence and activates a DNA damage response in normal fibroblasts induced to quiescence. Cell Cycle 8: 105-114, 2009.
61. Natallia L, Dama A, Gorica E, Darya K, Peña-Corona SI, Cortés H, Santini A, Büsselberg D, Leyva-Gómez G and Sharifi-Rad J: Genipin's potential as an anti-cancer agent: From phytochemical origins to clinical prospects. Med Oncol 41: 186, 2024.
62. Pan M, Luo M, Liu L, Chen Y, Cheng Z, Wang K, Huang L, Tang N, Qiu J, Huang A and Xia J: EGR1 suppresses HCC growth and aerobic glycolysis by transcriptionally downregulating PFKL. J Exp Clin Cancer Res 43: 35, 2024.
63. Sun K, Chen Y, Zheng S, Wan W and Hu K: Genipin ameliorates diabetic retinopathy via the HIF-1α and AGEs-RAGE pathways. Phytomedicine 129: 155596, 2024.
64. Kim BC, Kim HG, Lee SA, Lim S, Park EH, Kim SJ and Lim CJ: Genipin-induced apoptosis in hepatoma cells is mediated by reactive oxygen species/c-Jun NH2-terminal kinase-dependent activation of mitochondrial pathway. Biochem Pharmacol 70: 1398-1407, 2005.
65. Wang R, Shiu HT and Lee WYW: Emerging role of lncRNAs in osteoarthritis: An updated review. Front Immunol 13: 982773, 2022.